J Chem Crystallogr (2010) 40:624–629
DOI 10.1007/s10870-010-9707-9

ORIGINAL PAPER

Synthesis, Crystal Structure, and Rotational Energy Profile of 3-Cyclopropyl-1,2,4-benzotriazine 1,4-Di-*N*-oxide

Ujjal Sarkar · Rainer Glaser · Zack D. Parsons · Charles L. Barnes · Kent S. Gates

Received: 2 November 2009 / Accepted: 16 January 2010 / Published online: 5 February 2010

Abstract 1,2,4-Benzotriazine 1,4-di-*N*-oxides are potent antitumor drug candidates that undergo in vivo bioreduction leading to selective DNA damage in the low oxygen (hypoxic) cells found in tumors. Tirapazamine (TPZ) is the lead compound in this family. Here we report on the synthesis, crystal structure, and conformational analysis of a new analog, 3-cyclopropyl-1,2,4-benzotriazine 1,4-di-*N*-oxide (**3**). Compound **3** ($C_{10}H_{10}N_3O_2$) crystallized in the monoclinic space group *C2/c*. Unit cell parameters for **3**: $a = 16.6306$ (12), $b = 7.799$ (5), $c = 16.0113$ (11) Å, $\alpha = 90$, $\beta = 119.0440$ (10), $\gamma = 90$, and $z = 8$.

Keywords Crystal structure · *N*-oxide · Tirapazamine · Cyclopropyl group · Rotational energy profile

Introduction

3-Amino-1,2,4-benzotriazine 1,4-di-*N*-oxide (tirapazamine, TPZ, **1**) is currently undergoing a variety of phase I, II, and III clinical trials for the treatment of various human cancers [1, 2]. TPZ derives its medicinal activity by inducing DNA damage in poorly oxygenated tumor cells [3–18]. During the preclinical development of second generation analogues of TPZ it has become clear that 3-alkyl-1,2,4-benzotriazine 1,4-di-*N*-oxides have activities comparable to TPZ and may possess superior extravascular transport properties [9, 10]. Accordingly, we prepared 3-cyclopropyl-1,2,4-benzotriazine 1,4-dioxide (Scheme 1). An additional interesting aspect of compound **3** is that the cyclopropyl substituent has the potential to profoundly influence the reaction pathways available to the key radical intermediates generated in the bioactivation of 1,2,4-triazine 1,4-dioxides [3–18]. We report here the synthesis, X-ray crystal structure, and conformational analysis of this new 3-cyclopropyl-1,2,4-benzotriazine 1,4-dioxide (**3**). To the best of our knowledge this is the first 3-alkyl-1,2,4-benzotriazine 1,4-dioxide that has been crystallographically characterized. The crystal structure of **3** may contribute to understanding of the chemistry and biology of 3-cyclopropyl-1,2,4-benzotriazine 1,4-dioxide.

U. Sarkar · R. Glaser · Z. D. Parsons · C. L. Barnes · K. S. Gates (✉)
Department of Chemistry, 125 Chemistry Building, University of Missouri-Columbia, Columbia, MO 65211, USA
e-mail: gatesk@missouri.edu

K. S. Gates
Department of Biochemistry, University of Missouri-Columbia, Columbia, MO 65211, USA

Experimental

Oxidation of 3-Cyclopropyl-1,2,4-Benzotriazine (2) with *m*-Chloroperbenzoic Acid

To a solution of 3-cyclopropyl-1,2,4-benzotriazine **2** (50 mg, 0.25 mmol) in dichloromethane (10 mL), *m*-chloroperbenzoic acid (mCPBA, 2–6 equiv) was added and the resulting mixture stirred at room temperature until all starting material was consumed [21]. The solvent was then evaporated and the residue purified using gravity column chromatography on silica gel eluted with ethyl acetate-hexanes (1:1) to provide a 10–15% yield of **3** as deep yellow powder. ^{1}H-NMR ($CDCl_3$, 500 MHz): δ 8.55 (dd, $J = 8.5$, 1 Hz, 1H), 8.43 (dd, $J = 8.5$, 1 Hz, 1H), 8.00 (ddd, $J = 8.5$, 7, 1 Hz, 1H), 7.79 (ddd, $J = 8.5$, 7, 1 Hz, 1H), 3.14 (tt, $J = 8.0$, 5.0 Hz, 1H), 1.36 (m, 4H); ^{13}C-NMR (125 MHz, $CDCl_3$): δ 157.1, 139.0, 135.4, 133.9, 131.1, 121.5, 119.4,

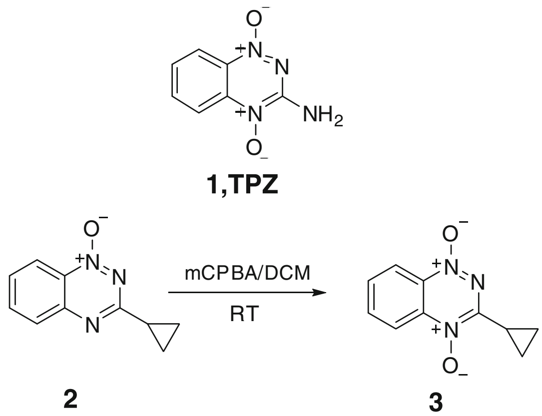

Scheme 1 Synthetic route for the preparation of 3-cyclopropyl-1,2,4-benzotriazine 1,4-di-*N*-oxide

10.1, 9.3; HRMS (ESI) *m/z* calc for $C_{10}H_{10}N_3O_2$ (M + H^+) 204.0773, found 204.0765.

Crystallography

Slow evaporation of dilute solutions of **3** in ethyl acetate-hexane afforded crystals suitable for X-ray diffraction analysis. Data was collected on Bruker SMART system at 173 K. Crystal structures were solved using SHELX programs [19, 20]. Details of the data collection and of the structure refinement are provided in Table 1.

Results and Discussion

Compound **3** crystallized in the monoclinic space group *C*2/*c*. Atomic coordinates and equivalent isotropic displacement parameters of the non-hydrogen atoms are given in Table 2, bond lengths and bond angles are shown in Tables 3 and 4, respectively, and an ORTEP drawing of **3** is shown in Fig. 1.

Figure 2 shows a diagram of packing viewed normal to the a–c plane. It can be seen that approximately coplanar molecules form layers along the a–c diagonal with considerable overlap of the aromatic rings. The final difference Fourier map shows peaks of electron density which appear to result from a minor contribution of a "whole body disorder" wherein the molecule is rotated normal to the approximate plane of the aromatic portion. This disordered component was not included in the final model.

Conformation and Rotational Energy Profile

The cyclopropyl group attached to a benzene ring adopts a bisected conformation, that is, the C–H bond of the

Table 1 Crystallographic data

	Compound **3**
Chemical formula	$C_{10}H_{10}N_3O_2$
CCDC no.	CCDC-752258
Color/shape	Yellow/prism
Formula weight	203.21
Crystal system	Monoclinic
Space group	*C*2/*c*
Temperature (K)	173 (2) K
Unit cell dimensions	$a = 16.6306(12)$ Å
	$b = 7.799(5)$ Å
	$c = 16.0133(11)$ Å
	$\alpha = 90°$
	$\beta = 119.0440(10)°$
	$\gamma = 90°$
Volume (Å^3)	1,815.8(2)
Z	8
Density (calculated) (mg/m^3)	1.494
Absorptioncoefficient (mm^{-1})	
Diffractometer/scan	Bruker SMART/CCD area detector
θ range for data collection (°)	2.8–27.13°
Reflections measured	6214
Independent/observed reflections	2005
Data/restraints/parameters	2005/0/140
Absorption correction	Semi-empirical
Goodness of fit on F^2	1.066
T_{min}, T_{max}	0.73, 0.98
Final *R* indices [$I > 2\sigma(I)$]	$R_1 = 0.0581$, $\omega R_2 = 0.1495$
R indices (all data)	$R_1 = 0.0721$, $\omega R_2 = 0.1614$

Table 2 Final coordinates and equivalent isotropic displacement parameters of the non-hydrogen atoms for compound **3**

Atom	*x*	*y*	*z*	*U* (eq) (Å^2)
O1	1,562	6,515	94	40
O4	2930	12320	1959	39
N1	1489	9327	187	32
N2	1911	7887	555	30
N3	2617	10892	1512	31
C1	1838	10786	655	31
C2	2735	7833	1431	25
C3	3170	6272	1796	30
C4	3992	6277	2635	37
C5	4380	7830	3109	39
C6	3939	9354	2760	35
C7	3099	9362	1911	27
C8	1345	12393	220	38
C9	317	12358	−388	34
C10	894	12598	−851	39

Table 3 Bond distances (Å) for compounds **3**

O(1)–N(2)	1.270(2)
O(4)–N(3)	1.289(2)
N(1)–N(2)	1.303(2)
N(1)–C(1)	1.331(3)
N(2)–C(2)	1.407(2)
N(3)–C(1)	1.357(3)
N(3)–C(7)	1.407(2)
C(1)–C(8)	1.474(3)
C(2)–C(7)	1.388(3)
C(2)–C(3)	1.391(3)
C(3)–C(4)	1.375(3)
C(3)–H(3)	0.9500
C(4)–C(5)	1.409(3)
C(4)–H(4)	0.9500
C(5)–C(6)	1.366(3)
C(5)–H(5)	0.9500
C(6)–C(7)	1.399(3)
C(6)–H(6)	0.9500
C(8)–C(9)	1.502(3)
C(8)–C(10)	1.509(3)
C(8)–H(8)	1.0000
C(9)–C(10)	1.479(3)
C(9)–H(9A)	0.9900
C(9)–H(9B)	0.9900
C(10)–H(10A)	0.9900
C(10)–H(10B)	0.9900

Table 4 Bond angles (°) for compounds **3**

N(2)–N(1)–C(1)	119.39(16)
O(1)–N(2)–N(1)	117.99(15)
O(1)–N(2)–C(2)	120.24(16)
N(1)–N(2)–C(2)	121.76(16)
O(4)–N(3)–C(1)	122.96(17)
O(4)–N(3)–C(7)	119.57(16)
C(1)–N(3)–C(7)	117.46(16)
N(1)–C(1)–N(3)	124.22(18)
N(1)–C(1)–C(8)	118.12(17)
N(3)–C(1)–C(8)	117.66(18)
C(7)–C(2)–C(3)	121.39(17)
C(7)–C(2)–N(2)	118.54(17)
C(3)–C(2)–N(2)	120.06(17)
C(4)–C(3)–C(2)	118.42(19)
C(4)–C(3)–H(3)	120.8
C(2)–C(3)–H(3)	120.8
C(3)–C(4)–C(5)	120.44(19)
C(3)–C(4)–H(4)	119.8
C(5)–C(4)–H(4)	119.8
C(6)–C(5)–C(4)	120.88(18)
C(6)–C(5)–H(5)	119.6
C(4)–C(5)–H(5)	119.6
C(5)–C(6)–C(7)	119.10(19)
C(5)–C(6)–H(6)	120.4
C(7)–C(6)–H(6)	120.5
C(2)–C(7)–C(6)	119.70(18)
C(2)–C(7)–N(3)	118.58(16)
C(6)–C(7)–N(3)	121.69(18)
C(1)–C(8)–C(9)	119.14(19)
C(1)–C(8)–C(10)	118.86(19)
C(9)–C(8)–C(10)	58.86(14)
C(1)–C(8)–H(8)	116.0
C(9)–C(8)–H(8)	116.0
C(10)–C(8)–H(8)	116.0
C(10)–C(9)–C(8)	60.84(15)
C(10)–C(9)–H(9A)	117.7
C(8)–C(9)–H(9A)	117.7
C(10)–C(9)–H(9B)	117.7
C(8)–C(9)–H(9B)	117.7
H(9A)–C(9)–H(9B)	114.8
C(9)–C(10)–C(8)	60.31(14)
C(9)–C(10)–H(10A)	117.7
C(8)–C(10)–H(10A)	117.7
C(9)–C(10)–H(10B)	117.7
C(8)–C(10)–H(10B)	117.7
H(10A)–C(10)–H(10B)	114.9

cyclopropyl carbon that is attached to the benzene ring is coplanar with the arene; $\tau = \angle(C_{ortho}–C_{ipso}–C_{CP}–H) = 0°$ [22]. In the bisected conformation the molecular orbital overlap between the cyclopropyl group and the arene π-system is maximal. The bisected conformation is exemplified, for example, by the crystal structures of cyclopropylbenzene [23, 24] and of cyclopropyl acetophenone [25].

Bisected structures also occur in heteroaryl-substituted cyclopropanes such as 2-cyclopropylpyridine [26] and, in such cases, there are two possible bisected conformations. In the case of heteroaryl cyclopropane **3**, the two conformational possibilities are characterized by $\tau = \angle(N1–C2–C_{CP}–H) = 0°$ and $\tau = 180°$, and the crystal structure analysis shows that the first of these options is realized in the solid ($\tau = 0°$).

Results of computational studies [27, 28] show that the conformation observed in the solid state also is the preferred conformation of free **3**. We explored the potential energy surface of **3** with density functional theory, B3LYP/6-31 + G(d), and also with second-order perturbation theory, MP2(full)/6-31 + G(d), and the rotational energy profiles are shown in Fig. 3. The DFT results are straightforward and they are as expected, that is, there are two minima **M1** ($\tau_1 = 0°$) and **M2** ($\tau_2 = 180°$) and **M1** is preferred over **M2** by $\Delta E_{rel} = 1.97$ kcal/mol. The rotational transition state structure **RTS** for rotation about the

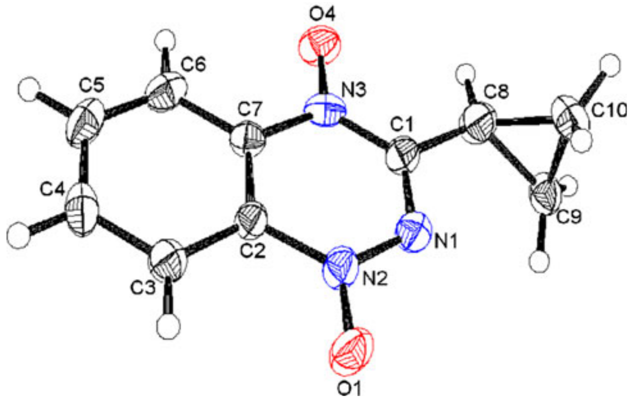

Fig. 1 ORTEP diagram of **3**

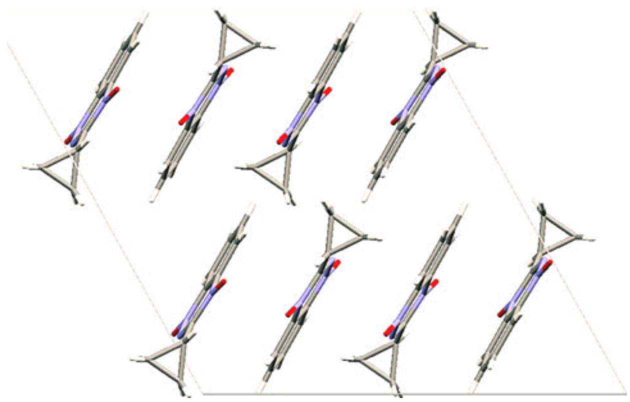

Fig. 2 Packing diagram of **3**

HAr–Cp bond also was located (Fig. 4) and the activation energies are ΔE(**M1** → **RTS**) = 6.16 and ΔE(**M2** → **RTS**) = 4.19 kcal/mol, respectively.

In each conformation, the C_{Cp}–H bond is pointed toward the lone pair region of one heteroatom (d(H–O_{N1}) = 2.327 Å in **M1**, d(H–N3) = 2.403 Å in **M2**) and the cyclopropyl-C_2H_4 moiety is placed close to the other (d(H–N3) = 2.672 Å in **M1**, d(H–O_{N1}) = 2.445 Å in **M2**). The sums of the van der Waals radii of H (1.20 Å) and of O (1.52 Å) or N (1.55 Å), respectively, are 2.72 and 2.75 Å, respectively. Hence, HAr–Cp bonding suffers from steric repulsion and the steric problems are less severe in **M1** (H–O_{N1} contact in 5-ring) than in **M2** (H–N3 contact in 6-ring). This repulsion is clearly manifest in the ∠(C2–CH–CH2) angles of **M1** (119.8°) and **M2** (125.2°). Driving the cyclopropyl-CH_2 moieties past O_{N1} is likely to be the major source of the rotational barrier; the **RTS** structure features (d(H–O_{N1}) = 2.359 Å and ∠(C2–CH–CH_2) angles of 125.5° and 119.5°.

The results obtained at the MP2 level are similar but also reveal some interesting new features. The comparison of the rotational energy profiles in Fig. 3 shows that the preference for **M1** is somewhat more pronounced at the

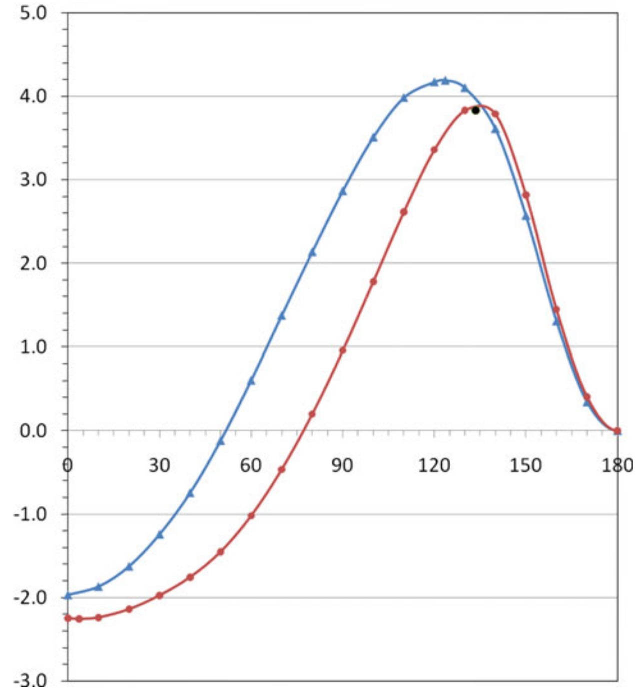

Fig. 3 Rotational profiles of **3** computed as a function of the dihedral angle $\tau = \angle(N_O\text{–}C\text{–}C_{CP}\text{–}H)$ at the theoretical levels B3LYP/6-31 + G(d) (blue) and MP2(full)/6-31 + G(d) (red). Energies are given in kcal/mol relative to the τ = 180° structure (**M2**)

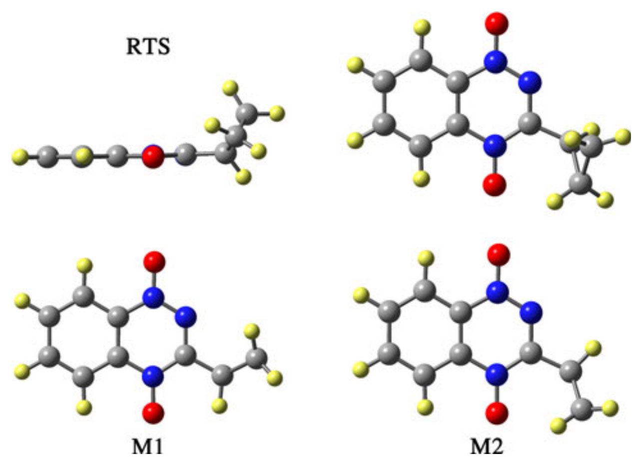

Fig. 4 B3LYP/6-31 + G(d) optimized structures of conformers **M1** and **M2** of **3** and of the rotational transition state structure **RTS** for their interconversion

MP2 level with ΔE_{rel} = 2.26 kcal/mol, and that the **RTS** structure is slightly shifted toward **M2**. While C_s-**M2** is a minimum at both theoretical levels, the minimum **M1** is not C_s-symmetric at the MP2 level and, instead, the optimized C_1-structure deviates ever so slightly from planarity (τ = 3.49°). An unexpected observation was made in the search for the **RTS** structure on the MP2(full)/6-31 + G(d) potential energy surface. The rotational energy profile scan provides a rather well defined expectation as to the location

Table 5 Computed isotropic magnetic shieldings and chemical shifts relative to TMS (in ppm) and spin–spin coupling constants J (in Hz)

Mol.	Nucleus	σ_{iso}	δ_{calc}	δ_{exp}	Computed J values	
M1	$H_u(CH)$	28.50	3.38	3.14 (tt)		
	$H_i(CH_2)$	30.65	1.23	1.36 (m)	$^3J(H_u,H_i) = 4.07$	$^3J(H_i,H_o) = 5.87$
	$H_o(CH_2)$	30.77	1.11		$^3J(H_u,H_o) = 8.24$	$^2J(H_i,H_o) = -3.72$
M2	$H_u(CH)$	29.86	2.02			
	$H_i(CH_2)$	29.22	2.66		$^3J(H_u,H_i) = 4.67$	$^3J(H_i,H_o) = 5.49$
	$H_o(CH_2)$	31.10	0.78		$^3J(H_u,H_o) = 8.62$	$^2J(H_i,H_o) = -3.32$
TMS	H	31.88	0.00			

[a] All values computed at the B3LYP/6-311 + G(2d,p) level

of the **RTS** structure and it should be routine to optimize the precise structure of the saddle point. Yet, even with excellent guesses of the initial structure and with the computation of the Hessian matrix at every point, searches for a stationary saddle point did not succeed. The black dot in the transition state region (Fig. 3) corresponds to a nonstationary near-**RTS** structure and it appears slightly below the red curve. There are many such "nonstationary near-**RTS** structures", they are essentially isoenergetic but differ in the specific combination of a great number of dihedral angles.

The results of the PES analysis are consistent with the measured ^{1}H-NMR spectrum and in particular with the cyclopropyl hydrogen signals at 3.14 (m, 1H) and 1.36 (m, 4H) ppm. For the dominant conformer **M1**, one would expect the unique cyclopropyl-H (H_u) to couple with two pairs of equivalent methylene hydrogens (H_i and H_o oriented toward and away from the heterocycle, respectively) and a tt-type splitting pattern should result ($^3J_{cis}(H_u,H_i)$, $^3J_{trans}(H_u,H_o)$) and such a multiplet is observed. The cyclopropyl methylene hydrogens of **M1** should give two signals for the hydrogens that are cisoid (H_o) or transoid (H_i) with the unique cyclopropyl hydrogen, and each signal should feature a ddd-type splitting pattern ($^3J_{cis}(H_u,H_o)$ or $^3J_{trans}(H_u,H_i)$, $^2J_{gem}(H_i,H_o)$, $^3J_{trans}(H_i,H_o)$). NMR computations require large, well-polarized basis sets and we computed isotropic magnetic shielding and spin–spin coupling constants for **M1** and **M2** using the GIAO method at the B3LYP/6-311 + G(2d,p) level [29–31]. The computed shielding values are reported relative to TMS in parts per million (ppm) and computed J values are reported in Hertz (Hz). The data in Table 5 support the conclusion that the preferred gas phase conformer also is preferred in solution. The chemical shifts computed for **M1** closely match the observed spectrum whereas those computed for **M2** do not. First-order analysis of the H_u signal results in coupling constants of 8 and 5 Hz and these values are in good agreement with the computed coupling constants $^3J(H_u,H_i)$ and $^3J(H_u,H_o)$.

Conclusion

In conclusion, we found that the solid state conformation of **3** also is the preferred conformation in the gas phase and in solution. The crystallographic characterization of 1,2,4-benzotriazine di-*N*-oxide may be relevant to the properties of the 3-cyclopropyl-1,2,4-benzotriazine 1,4-dioxide radical where conformational isomerism will affect potential ring opening reactions.

Supplementary Material

X-ray crystallographic data have been deposited with the Cambridge Crystallographic Data Center as supplementary publication number CCDC 752258. Copies of available material can be obtained, free of charge, on application to the Director, CCDC, 12 Union Road, Cambridge CB21EZ, UK.

Acknowledgments We thank National Institutes of Health (CA 100757) for support of this work. MU Research Computing is supported by Federal Earmark NASA Funds for Bioinformatics Consortium Equipment and additional support from Dell, SGI, Sun Microsystems, TimeLogic and Intel.

References

1. Marco L, Olver I (2006) Curr Clin Oncol 1:71–79
2. Le Q-TX, Moon J, Redman M, Williamson SK, Lara PN Jr, Goldberg Z, Gaspar LE, Crowley JJ, Moore DF Jr, Gandara DR (2009) J Clin Oncol 27:3014–3019
3. Horsman MR (1998) Int J Radiat Oncol Biol Phys 42:701–704
4. Siemann DW (1998) Int J Radiat Oncol Biol Phys 42:697–699
5. Vaupel P, Kallinowski F, Okunieff P (1989) Cancer Res 49:6449–6465
6. Brown JM, Wilson WR (2004) Nat Rev Cancer 4:437–447
7. Brown JM (1999) Cancer Res 59:5863–5870
8. Zeman EM, Brown JM, Lemmon MJ, Hirst VK, Lee WW (1986) Int J Radiat Oncol Biol Phys 12:1239–1242
9. Hay MP, Hicks KO, Pruijn FB, Pchalek K, Siim BG, Wilson WR, Denny WAJ (2007) Med Chem 50:6392–6404

10. Hay MP, Pchalek K, Pruijn FB, Hicks KO, Siim BG, Anderson RF, Shinde SS, Phillips V, Denny WA, Wilson WRJ (2007) Med Chem 50:6654–6664
11. Chowdhury G, Junnutula V, Daniels JS, Greenberg MM, Gates KSJ (2007) Am Chem Soc 129:12870–12877
12. Birincioglu M, Jaruga P, Chowdhury G, Rodriguez H, Dizdaroglu M, Gates KSJ (2003) Am Chem Soc 125:11607–11615
13. Kotandeniya D, Ganley B, Gates KS (2002) Bioorg Med Chem Lett 12:2325–2329
14. Daniels JS, Gates KS, Tronche C, Greenberg MM (1998) Chem Res Toxicol 11:1254–1257
15. Junnotula V, Sarkar U, Sinha S, Gates KSJ (2009) Am Chem Soc 130:1015–1024
16. Daniels JS, Gates KSJ (1996) Am Chem Soc 118:3380–3385
17. Anderson RF, Shinde SS, Hay MP, Gamage SA, Denny WAJ (2003) Am Chem Soc 125:748–756
18. Shinde SS, Hay MP, Patterson AV, Denny WA, Anderson RF (2009) J Am Chem Soc 131:14220–14221
19. Sheldrick GM (1997) SHELXS-97, program for the solution 125 of crystal structures. University of Gottingen, Germany
20. Sheldrick GM (1997) SHELXS-97, program for the refinement 128 of crystal structures. University of Gottingen, Germany
21. Fuchs T, Gates KS, Hwang J-T, Greenberg MM (1999) Chem Res Toxicol 12:1190–1194
22. de Boer JSAM, Loopstra BO, Stam CH (1987) Red Trau Chim Pays-Bas 106:537
23. Shen Q, Wells C, Traetteberg M, Bohn RK, Willis A, Knee J (2001) J Org Chem 66:5840–5845
24. Bernal I, Levendis DC, Fuchs R, Reisner GM, Cassidy JM (1997) Struct Chem 84:275–285
25. Drumright RE, Mas RH, Merola JS, Tanko JMJ (1990) Org Chem 55:4098–4102
26. Traetteberg M, Rauch K, de Meijere A (2005) J Mol Struct 738:25–31
27. Cramer CJ (2004) Essentials of computational chemistry. New York, Wiley
28. Frisch MJ, Trucks GW, Schlegel HB, Scuseria GE, Robb MA, Cheeseman JR, Montgomery JA Jr, Vreven T, Kudin KN, Burant JC, Millam JM, Iyengar SS, Tomasi J, Barone V, Mennucci B, Cossi M, Scalmani G, Rega N, Petersson GA, Nakatsuji H, Hada M, Ehara M, Toyota K, Fukuda R, Hasegawa J, Ishida M, Nakajima T, Honda Y, Kitao O, Nakai H, Klene M, Li X, Knox JE, Hratchian HP, Cross JB, Bakken V, Adamo C, Jaramillo J, Gomperts R, Stratmann RE, Yazyev O, Austin AJ, Cammi R, Pomelli C, Ochterski JW, Ayala PY, Morokuma K, Voth GA, Salvador P, Dannenberg JJ, Zakrzewski VG, Dapprich S, Daniels AD, Strain MC, Farkas O, Malick DK, Rabuck AD, Raghavachari K, Foresman JB, Ortiz JV, Cui Q, Baboul AG, Clifford S, Cioslowski J, Stefanov BB, Liu G, Liashenko A, Piskorz P, Komaromi I, Martin RL, Fox DJ, Keith T, Al-Laham MA, Peng CY, Nanayakkara A, Challacombe M, Gill PMW, Johnson B, Chen W, Wong MW, Gonzalez C, Pople JA (2004) Gaussian 03, revision D.01. Gaussian Inc., Wallingford
29. Cheeseman JR, Trucks GW, Keith TA, Frisch MJJ (1996) Chem Phys 104:5497–5509
30. Alkorta I, Elguero J (2003) Struct Chem 14:377–389
31. Deng W, Cheeseman JR, Frisch MJ (2006) J Chem Theory Comput 2:1028–1037